Variations in Sediment Strength across a Sandy Peninsula

Nicola C. Brilli[1] and Nina Stark, Ph.D., M.ASCE[2]

[1]Virginia Tech, Dept. of Civil and Environmental Engineering, Blacksburg, VA. E-mail: nickb96@vt.edu
[2]Virginia Tech, Dept. of Civil and Environmental Engineering, Blacksburg, VA. E-mail: ninas@vt.edu

ABSTRACT

Phipps Peninsula is a sandy peninsula located near the town of Yakutat, Alaska. In the summer of 2018, a field study was conducted in three areas of the peninsula. All three locations feature complex sediment remobilization processes shaping the local geomorphology. Here, variations in geotechnical properties at the three test sites are investigated. For this purpose, a portable free fall penetrometer (PFFP) was deployed along several transects at the three sites, totaling approximately 750 deployments throughout the course of the study. Since field studies using PFFP on sub-aerial and intertidal beach areas are limited, and results are highly variable, novel methods were implemented for the analysis of the PFFP data. This study represents a first step towards the use of PFFP data to characterize geotechnical properties on sub-aerial and intertidal beaches. Temporal differences in strength are discussed in the context of local physical processes, and spatial variability was related to differences in morphology and hydrodynamics.

INTRODUCTION

Sediment strength (e.g., in terms of bearing capacity and/or shear strength) is an important consideration for many coastal applications, including assessing beach trafficability and understanding local sediment transport/remobilization processes. However, coastal environments present unique challenges for measuring sediment strength. Nearshore areas are often highly energetic and beach environments can be affected by dynamic geomorphodynamics. This makes the use of the heavy equipment typical to geotechnical surveying impractical in these areas and sometimes unsuitable to test near-surface sediments. In the nearshore zone, portable free-fall penetrometers (PFFPs), which are low-cost, lightweight, and easily deployable from a small craft, enable a geotechnical characterization of surficial subaqueous sediments in energetic coastal environments (Stark et al. 2014a). For sandy nearshore sediments, analysis of PFFP data can provide an estimate of equivalent cone resistance (Akal and Stoll 1995; Stoll et al. 2007; Stark et al. 2009, 2012; Lucking et al. 2017), relative density, and friction angle (Albatal et al. 2019) using deceleration measurements. However, this work has rarely been extended onto the sub-aerial and intertidal (exposed to the air, not submerged) beach areas (Reeve et al. 2018). An added complexity of using PFFP on beaches stems mainly from the effects of partial saturation, which introduces an apparent cohesion adding to the sediment strength that may change with time (Lu and Likos 2006, 2013). Other factors affecting local sediment strength include complex groundwater-swash zone interaction (Heiss et al. 2014, 2015) and spatiotemporal variations in geomorphology and sediment distributions in response to tidal variations and hydrodynamic forcing (Masselink et al. 2006; Sassa and Watabe 2007, 2009). As an initial step towards extending the use of PFFPs into sub-aerial and intertidal beach environments, this paper aims to examine the strength data obtained from PFFP deployments at three beaches, analyze temporal differences in strength along a crosshore transect, and discern if hydrodynamic and

morphodynamic differences can explain differences in strength profiles at three distinct sites.

REGIONAL CONTEXT

This study was performed on Phipps Peninsula, a sandy peninsula west of the town of Yakutat, Alaska. Yakutat is located about 225 miles northwest of Juneau, and Phipps Peninsula is bordered by the Gulf of Alaska to the southwest, Yakutat Bay to northwest, and Monti Bay to the northeast. Figure 1 shows the overall area and the location of the three study sites. The following sections will detail the local geology, geomorphology, and hydrodynamic conditions of the three different sites.

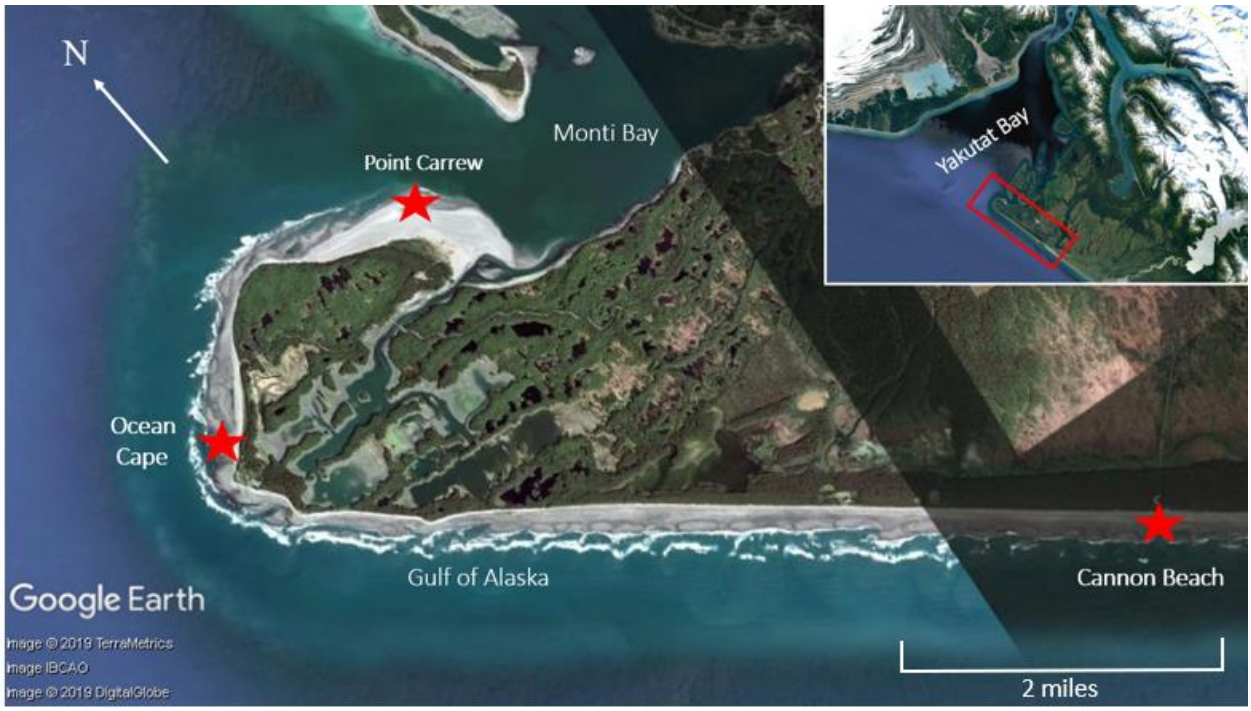

Figure 1: Site Geography and Study Locations, *Source:* "Yakutat" 59°32'33.01"N and 139°49'35.74"W. Google Earth. May 11, 2016.

Geology: All three test sites are composed of predominantly fine quartz sand, having a dark color due to the presence of heavy minerals. Cannon Beach was the only site characterized by an appreciable increase in median grain size (d_{50}) along a crosshore profile, increasing from 230 μ m to 310 μm from the dune towards the low water line. Sediment distributions at Ocean Cape and Point Carrew were more uniform, with a median grain size of 260 μ m. Ocean Cape features additionally a large boulder field located on a low-tide terrace, likely due to local erosion of the headland, which was not surveyed in this study. The Yakutat area is seismically active. Thus, the beaches have the potential for liquefaction and/or impacts of submarine landslides during earthquakes (Yehle 1971).

Morphology: Cannon Beach is wide (150 m) and has the most gently sloping intertidal zone (3°) of the three beaches tested, Ocean Cape is much narrower (80 m) and steeper (5°), and Point Carrew is a very wide sandy spit (460 m), also with a steeper intertidal zone (5°) (Table 1). Ridge-runnel systems (King and Williams 1949) were observed at all three sites, but the crosshore transect at Cannon Beach did not capture this feature at the time of measurements.

Table 1: Morphology Summary

Site	Low-Tide Beach Width (meters)	Intertidal Slope (degrees)
Cannon Beach	150	3.1
Ocean Cape	80	5.1
Point Carrew	460	5.0

Hydrodynamics: Exposed to swell from the Gulf of Alaska, Cannon Beach features the overall highest wave energy of the three sites, with the predominant wave direction from the south. Ocean Cape is exposed to similar hydrodynamic conditions as Cannon Beach, being located at the headland between the Gulf of Alaska and Yakutat Bay. The annual average significant wave height for these two sites is 1.9 m at the 10 m depth contour (Previsic and Bedard 2009). The wave climate drives strong longshore sediment transport along the beach to the north. Here, the waves refract around the peninsula, depositing sediment and forming the spit at Point Carrew. Point Carrew is sheltered from the ocean swell, facing northeast on Monti Bay, and has an average significant wave height of 0.5 m at 10 m depth. The average annual wave height 50 km offshore is 2.5 m (Previsic and Bedard 2009).

METHODS

Two to three (eight in total) cross-shore transects were investigated at each site over a 6-day period. The PFFP *blueDrop* (Stark et al. 2014b) was deployed three times at each station along the cross-shore profiles. The device is of streamlined torpedo-like shape, 63.1 cm long, and has a mass of 7.71 kg. It is equipped with five vertical microelectromechanical systems (MEMS) accelerometers, two horizontal MEMS accelerometers, a pressure transducer, which was not utilized for this study, and a conical steel tip. The accelerometers can measure ±1.7-250 *g* in the vertical, and ±55 *g* (*g* is gravitational acceleration) in the horizontal to determine tilt. The device was released about 1 m above the sediment surface, which is high enough for the probe to obtain an impact velocity of 4-5 m/s while not tiring the operator. It fell freely through air, and then penetrated the sediment, being brought to a stop by the sediment resistance. The accelerometers, recording continuously at 2 kHz, captured the full acceleration-deceleration profile at a sub-centimeter vertical resolution once double-integrated. Using Newton's 2nd Law, the deceleration profile from impact to stop is converted into a sediment resistance force, and then into a dynamic bearing capacity or cone resistance considering the cone area. The equivalent of a quasi-static bearing capacity (*qsbc*) is then estimated by applying a strain rate correction to normalize to a constant velocity (2 cm/s) following Dayal and Allen (1973). The underlying assumptions and detailed explanation of the process to acquire a *qsbc* profile from the deceleration profile is provided in Stark et al. (2012). While there is uncertainty related to the strain rate correction factor, K, Albatal et al. (2019) found good agreement using $K = 0.3$ for sands from this region. This value was therefore adopted here as well. Finally, integrating the deceleration profile can provide the impact velocity, and double-integration provides the penetration depth (Dayal and Allen 1973; Stoll and Akal 1999; Stark and Wever 2009). Time constraints prevented independent measurements of penetration depth at every deployment locations, but the derived penetration depth was confirmed by occasional measurements and available photo materials. The pressure sensor was not utilized here due to limited penetation depths (often < 7.5 cm, thus, the pressure transducer ports have not been embedded in the soil) and a complex pore pressure response to partially saturated sediments that was out of the scope of this article. Over the course of the study, the PFFP was deployed 753 times along the eight transects.

Other field methods included: sediment sampling along each transect at PFFP deployment locations to obtain moisture contents and bulk densities, simplistic topographic profiling to measure beach slopes and small-scale temporal morphological change, and recording of wave heights by anchoring an *RBR Solo* pressure sensor in the beach face. Over 300 sediment samples were weighed and oven-dried, and pressure sensors were deployed over several tidal cycles to accurately represent the wave climate.

RESULTS

Beach Profiles: Topographic profiles measured at each location are provided as visual aid to explain the differences in morphology and as support for discussion (Figure 2).

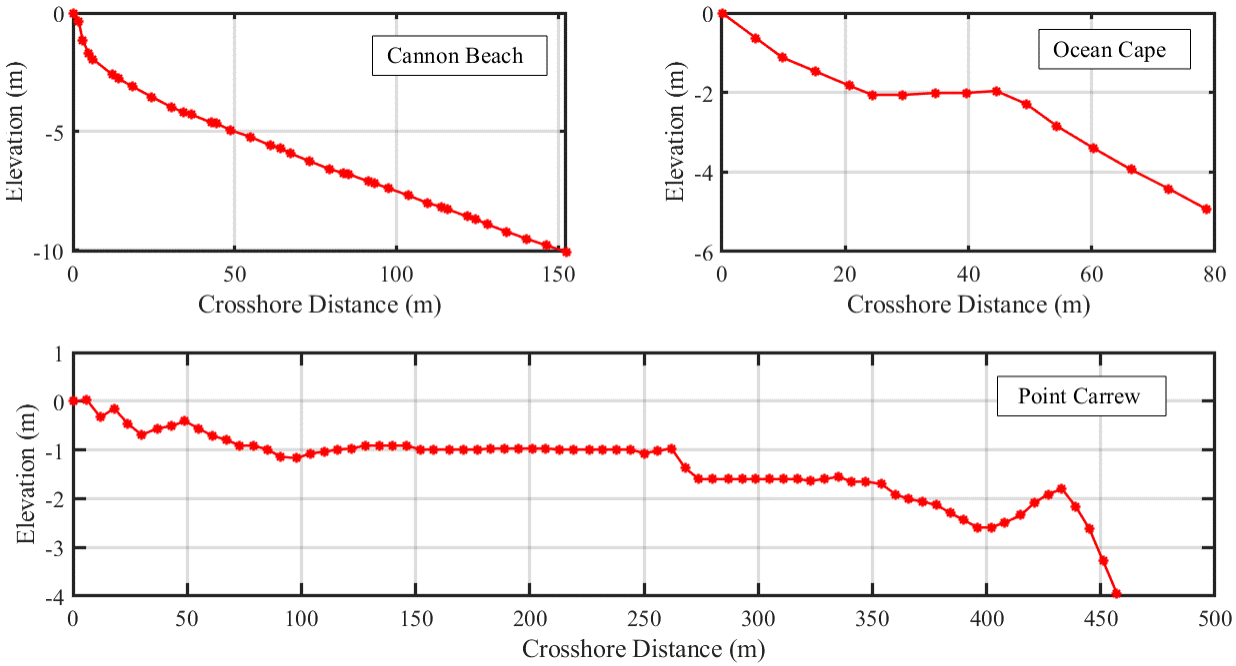

Figure 2: Topographic profiles at Cannon Beach (Top Left), Ocean Cape (Top Right), and Point Carrew (Bottom), Point Carrew profile adapted from Stark et al. (2019). The beginning of each profile (0m crosshore distance) corresponds to the toe of the dune.

Penetrometer Deployments: High variability of the PFFP profiles was observed (Figure 3). The profiles were grouped into three general types, based on their shape with sediment depth. Type A profiles (Figure 3 left) resembled the typical strength profile shape found by Albatal and Stark (2016) for sediments just offshore of Phipps Peninsula, and were seen predominantly for penetration depths greater than 10 centimeters. They feature low strengths in the upper 5 cm of the profile, followed by an increase in strength with depth until reaching a maximum, after which the decrease is due to the penetrometer coming to a stop. Type B profiles (Figure 3 center) exhibited an approximately constant sediment strength with depth, lacked a well-defined maximum, and were typical of penetration depths of 7-10 centimeters (slightly deeper than the cone height). Type C (Figure 3 right) profiles were observed for deployments in the swash zone of the beach where the penetration depth was less than 7 centimeters (less than the cone height). The observed decrease in strength could be due to the probe falling over. It is important to note that the maximum *qsbc* increased from Type A to C, ranging from 50-500 kPa. For profiles

resembling the Type A shape, the maximum *qsbc* is often compared to investigate spatiotemporal variations (Albatal and Stark 2016). However, defining a consistent strength from maximum value becomes difficult when Type A, B, & C profiles were all observed along the same transect. Therefore, it was decided to use the *qsbc* at 4 centimeters of penetration depth as a comparable sediment strength between all deployments. This depth was chosen because all deployments reached at least 4 centimeters, giving a surficial strength for every deployment, and this decision allowed for a consistent comparison between otherwise varying results. It should be noted that this choice of depth is somewhat arbitrary, and could vary for different sites, based on the range of penetration depths present in the data set.

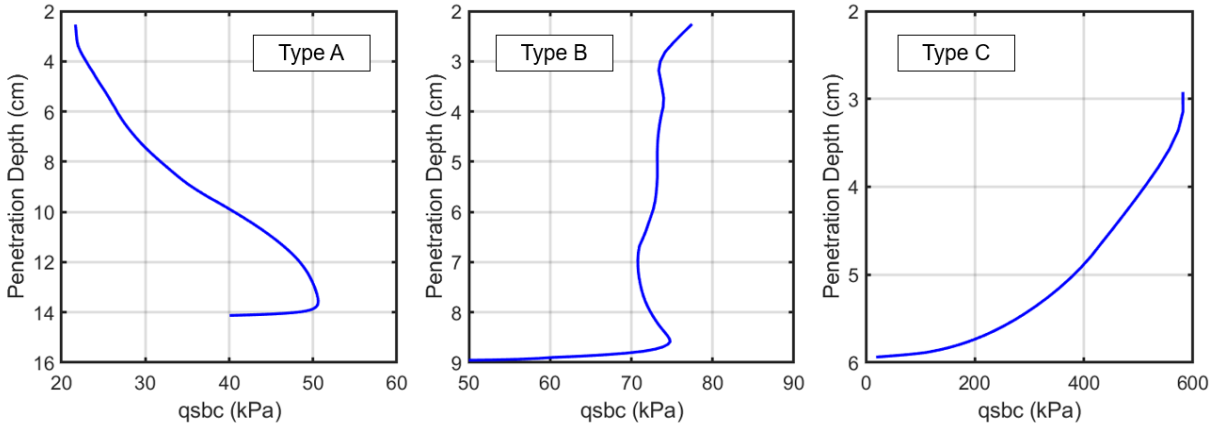

Figure 3: Variability in PFFP profiles: (Left) Type A – increasing strength with depth, defined maximum, & penetration > 10 cm, (Center) Type B – constant strength with depth, lack of defined maximum, penetration 7-10 cm , (Right) Type C – swash zone deployments, highest strength magnitudes, penetration < 7 cm

Temporal Variations at Cannon Beach: Transects were tested at Cannon Beach every twelve hours during daylight over the course of two full tidal cycles, capturing three low tides. This allowed for a temporal comparison of the strength profiles (Figure 4). Within the dry zone of the beach above the high tide mark (from the dune at 0 m out to 40 m), there was little variability in the sediment strength. However, this changed drastically in the intertidal zone with profiles fluctuating from 50 – 300 kPa. The intertidal zone is the area of the beach between the high tide line and the low water line. The emerged width of this zone changes throughout the tidal cycle, being smallest at high tide and widest at low tide. All transects displayed a large increase in strength approaching the swash zone. It is important to note the order of magnitude of difference in sediment strength along the profiles, with the dry zone being on the order of tens of kPa and the intertidal/swash zone going up to hundreds of kPa.

Spatial Variations between the Sites: To compare the different sites, strength profiles were selected for transects that were surveyed at the same point on the tidal cycle, just after low tide, and plotted versus the non-dimensional distance along the total transect length, *L*, to place transects of different lengths on the same scale (Figure 5). All three sites exhibited similar magnitudes of strength in the dry (sub-aerial) zone, and all three featured a spike in strength at the end of the profile that corresponded to the swash zone. Cannon Beach was the only site to show variability in the intertidal zone (it also has the largest intertidal zone of the three sites). Ocean Cape did not show intertidal variability but did show a similar increase in strength approaching the swash zone. Point Carrew represented a long consistent profile, and showed a

strength increase at the swash zone that was less than at the other two sites. Ocean Cape and Point Carrew each exhibited a small decrease in strength right before the increase at the swash, which was not seen on the Cannon Beach profile.

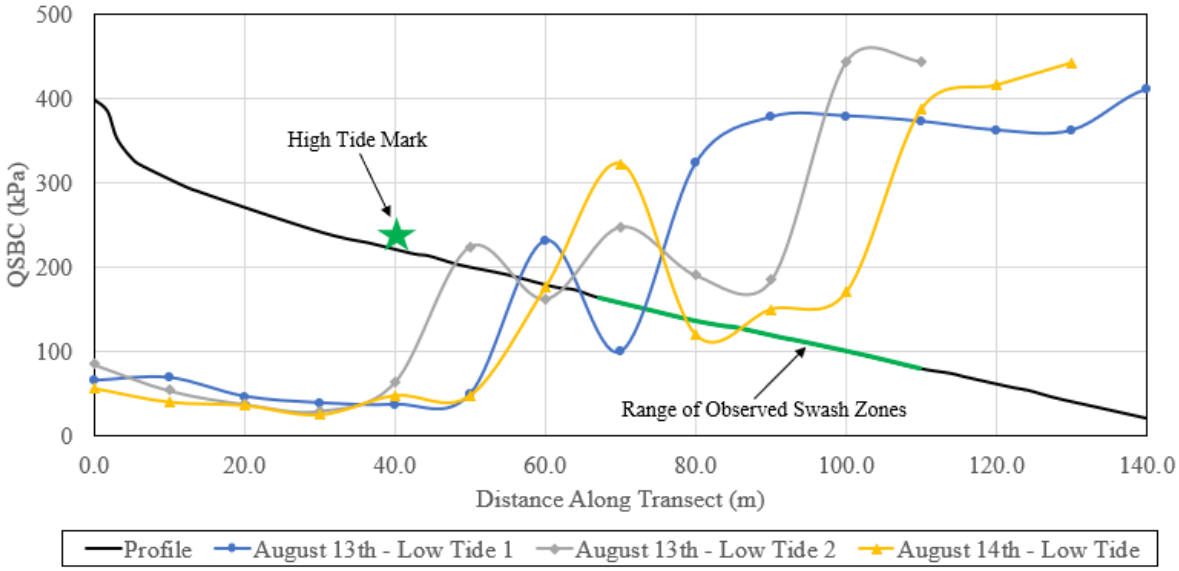

Figure 4: Strength profiles from 3 low tides at Cannon Beach. Green star marks the high tide line which is the extent of the dry zone. The green line on the topographic profile shows the extent of the fluctuations of the swash zone during measurements.

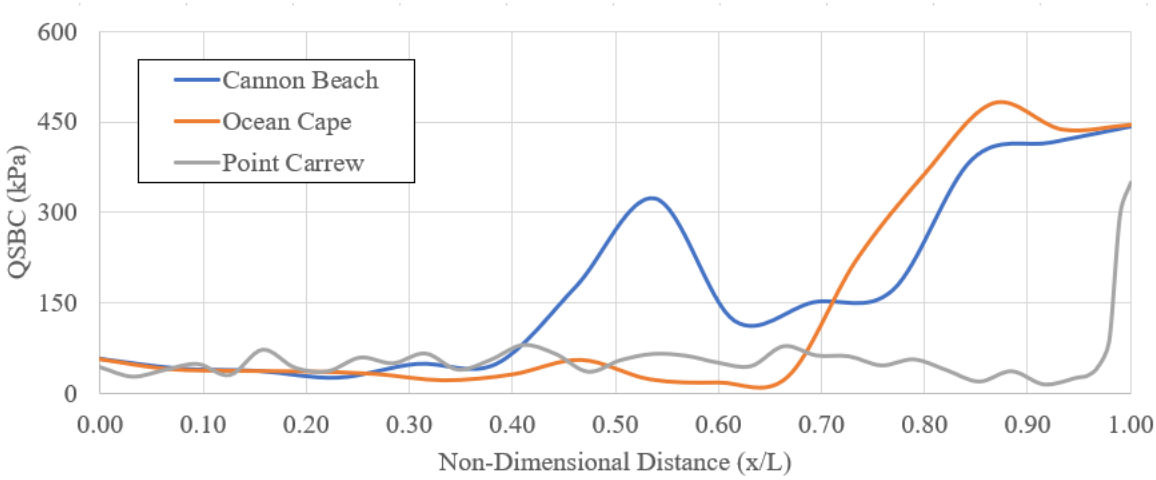

Figure 5: Strength profiles along transects for the three sites near low tide. Cannon Beach shows fluctuation within intertidal zone and Ocean Cape lacks this variability. Point Carrew has a very wide dry zone, but all three increase approaching the swash.

DISCUSSION

Temporal Variations at Cannon Beach: The consistency of strength in the dry (sub-aerial) zone for all four measurement times matched expectations (Figure 4). This area is above the high tide line and the water table, and such, it is not subject to daily fluctuations in water content or density. However, it rained during all four measurement times. This introduced somewhat of water content across the beach, but this effect was approximately consistent for all

measurements, and thus, is not expected to affect the comparison. All profiles show a large increase in strength approaching the swash zone, which was also seen by Reeve et al. (2018). This increase can be tied to reworking of sediments due to swash and backwash processes and porosity reduction over time due to wave action. (Heathershaw 1981; Dean and Dalrymple 2004). As waves break and disturb the sediment bed, the induced swash could remove any loose sediments, leaving only the denser, stronger, less erodible sediments behind. Shear stresses can also contribute to particle rearrangement and densification.

The intertidal zone at Cannon Beach is very wide (~100 meters) which means that large portions of the beach are cyclically submerged and drained throughout the tidal cycle. The swash zone at any given time during the tidal cycle appears to be subject to sediment strengthening processes mentioned previously. Yet, the entire intertidal zone does not display such high strengths, only the swash zone. Thus, the same processes that serve to strengthen the sediment in the swash zone cannot account solely for the high variability seen in the intertidal zone. As the tide goes in and out each day, sediment is constantly being moved and reworked by the waves and currents. Loose sediments eroded by the waves are deposited elsewhere on the beach, and as the location of the swash zone changes so does the location of high strength. Thus, this implies an inherent spatial variability of sediment strength in the intertidal zone. Furthermore, as sections of beach emerge as the tide retreats, the beach face must drain, leaving zones of partially saturated soil, which is another source of strength (Lu and Likos 2006, 2013, Lu et al. 2009). With the large tidal variation seen at this site (~3 meters), the effects of groundwater table fluctuations likely act to complicate drainage and partial saturation (Heiss et al. 2014, 2015).

In summary, the dry zone was temporally consistent in strength due to being above the high tide line and the groundwater table, the swash zone is consistently higher in strength due to active localized wave action and swash processes, and the intertidal zone is highly variable due to deposition/erosion throughout the tidal cycle and complex groundwater/partial saturation effects. The processes contributing to high variability in the intertidal zone are only described here as potentially causing changes in the sediment strength, and future work will need to be conducted to adequately quantify such changes.

Spatial Variations. In the surveyed areas of the three sites, Cannon Beach featured a slight increase in grain size towards the water, while Ocean Cape and Point Carrew were characterized by uniform grain sizes. At Ocean Cape, a large cobble and boulder field eas observed below the survey site. The increase in grain size along the transect is consistent with the literature (Abuodha 2003), and Duncan, Wright, & Brandon (2014) noted an increase in shear strength with grain size of sands, gravels, and rockfills as well as between well-graded and poorly-graded sands. However, the effects of these differences unlikely explain alone the high range of strengths seen in the profiles. Thus, grain size is not a large contributor to differences in strength between the sites. The gravel and boulder field seen on the low tide terrace of Ocean Cape may have effects on the sediment transport processes between the nearshore and intertidal, which could in turn have effects on the measured strengths, but since this area was not surveyed, such effects are outside the scope of this study, and will be considered in future work.

Cannon Beach featured no distinct morphological bedforms but an approximately constant intertidal beach slope at the time of measurements (Figure 2 Left). Nevertheless, it has the highest amount of intertidal variability in strength (Figure 5). The reason that the other two sites, which also have intertidal zones affected by the same processes, do not show such variability is tied to the morphology. The transects at Ocean Cape and Point Carrew both exhibited a ridge-runnel profile in the intertidal zone at the time of measurements (King and Williams 1949).

When surveyed at low tide, the runnel is filled with water and the ridge is exposed. From the top of the ridge, the beach then again slopes back down to the swash zone and water line. (Figure 2, Right & Bottom). In Figure 5, there is a small decrease in strength just before the large increase in strength in both the Ocean Cape and Point Carrew profiles. This decrease is consistent with the location of the water-filled runnel. The sand in the runnel is fully saturated and loose due to being fully submerged and constantly reworked by flows within the channel and the morphodynamics of intertidal bar systems (Masselink et al. 2006). The subsequent increase would then be due to partial saturation effect increasing the strength on the exposed ridge, and the small intertidal zones at both sites putting the swash zone just below the ridge. Finally, the majority of the Point Carrew profile represents the sub-aerial zone. The typical increase in strength is seen at the swash zone, but to a lesser extent than the other two sites (Figure 5). The waves that reach Point Carrew must refract around the tip of the peninsula, causing them to become smaller and lose energy (Dean and Dalrymple 2004). Since the wave energy is lower at Point Carrew, the strength increase from densification is lessened at this site. The three sites are different morphologically, and these differences are in line with the strength differences. Still, more research is needed to quantify the effects of hydrodynamic processes on the measured sediment strengths.

CONCLUSIONS

A portable free-fall penetrometer was deployed at three sites on a sandy peninsula to explore the use of PFFP's in sub-aerial and intertidal coastal environments. Additional goals of the study were to assess the temporal and spatial differences in sediment strength between the sites, using the obtained geotechnical properties. Cannon Beach is a wide, high energy beach with no morphological features at the time of measurements, Ocean Cape is a narrow, high energy beach, with a ridge-runnel system, and Point Carrew is a very wide spit, also with a ridge-runnel, but with low wave energy due to being on a protected bay. Lack of consistency in results of PFFP deployments along beach transects motivated using the strength at 4 centimeters of penetration depth as the sediment strength for comparison between all deployments. Temporal variations at Cannon Beach were explained by a number of interacting processes: in-situ densification from waves and swash, partial saturation over tidal cycles, and groundwater table fluctuation. Quantifying the effects of these processes will be the subject of future work. Finally, the differences in strength along transects between the sites were explained by the differences in morphology and hydrodynamics, namely the presence of ridge-runnel systems and differences in wave energy.

ACKNOWLEDGMENTS

The authors acknowledge funding by the National Science Foundation through grant CMMI-1751463. The authors also acknowledge funding for travel support of undergraduate researchers who contributed to the data collection by Dr. Mike Duncan. Furthermore, the authors would like to thank Julie Paprocki, Dennis Kiptoo, and the undergraduate students of the Coastal Geotechnical Field Research Experience 2018 for support in the field. The authors would also like to thank the City and Borough of Yakutat, and specifically, Rhonda Coston and Irving Grass, and the Yakutat Lodge for local support.

REFERENCES

Abuodha, J.O.Z. (2003). "Grain size distribution and composition of modern dune and beach sediments, Malindi Bay coast, Kenya." *J. Afr. Earth Sci.,* 36, 41–54.

Akal, T., and Stoll, R. D. (1995). "An expendable penetrometer for rapid assessment of seafloor parameters." OCEANS 1995. *MTS/IEEE, Challenges of Our Changing Global Environment*., IEEE, San Diego, CA, 1822–1826.

Albatal, A. and Stark, N. (2016). "In Situ Geotechnical Early Site Assessment of a Proposed Wave Energy Converter Site in Yakutat, Alaska, Using a Portable Free-Fall Penetrometer." *Proc., Geo-Chicago 2016*, ASCE, Reston, VA ,429-438.

Albatal, A., Stark, N., and Castellanos, B. (2019). "Estimating in-situ relative density and friction angle of nearshore sand from portable free fall penetrometer tests." *Canadian Geotechnical Journal.* 0(ja).

Dayal, U., and Allen, J. H. (1973). "Instrumented Impact Cone Penetrometer." *Canadian Geotechnical Journal*, 10(3), 397–409.

Duncan, J. M., Wright, S. G., and Brandon, T. L. (2014). *Soil strength and slope stability*. John Wiley & Sons, Hoboken, NJ.

Dean, R. G., and Dalrymple, R. A. (2004). *Coastal processes with engineering applications*. Cambridge University Press.

Heathershaw, A.D., Carr, A.P., Blackley, M.W.L., and Wooldridge, C.F. (1981). "Tidal variations in the compaction of beach sediments." *Marine Geology,* 41, 223 – 238.

Heiss, J. W., Ullman, W. J., & Michael, H. A. (2014). Swash zone moisture dynamics and unsaturated infiltration in two sandy beach aquifers. *Estuarine, Coastal and Shelf Science*, 143, 20-31.

Heiss, J. W., Puleo, J. A., Ullman, W. J., & Michael, H. A. (2015). Coupled surface-subsurface hydrologic measurements reveal infiltration, recharge, and discharge dynamics across the swash zone of a sandy beach. *Water Resources Research*, 51(11), 8834-8853.

King, C.A.M., and Williams, W.W. (1949). "The formation and movement of sand bars by wave action." *Geographical Journal 113*, 70–85.

Lu, N., and Likos, W.J. (2006). "Suction Stress Characteristic Curve for Unsaturated Soil." *Journal of Geotechnical and Geoenvironmental Engineering,* 132(2), 131-142.

Lu, N. and Likos, W.J. (2013). "Origin of Cohesion and Its Dependence on Saturation for Granular Media." *Poromechanics V*, 669-675.

Lucking, G., Stark, N., Lippmann, T., and Smyth, S. (2017). "Variability of in situ sediment strength and pore pressure behavior of tidal estuary surface sediments." *Geo-Marine Letters*, 37(5), 441-456.

Masselink, G., Kroon, A., and Davidson-Arnott, G.D., (2006). "Morphodynamics of intertidal bars in wave-dominated coastal settings — A review." *Geomorphology,* 73(1), 33-49.

Previsic, M., and Bedard, R. (2009). Yakutat Conceptual Design, Performance, Cost and Economic Wave Power Feasibility Study. Tech. Report No. EPRI-WP-006-Alaska.

Reeve, B., Stark, N., and Mewis, P. (2018). "Cross-shore variations in sediment strength at a sandy beach." *Proc. Coastal Engineering,* 36.

Sassa, S., & Watabe, Y. (2007). Role of suction dynamics in evolution of intertidal sandy flats: Field evidence, experiments, and theoretical model. *Journal of Geophysical Research: Earth Surface*, 112.

Sassa, S. and Watabe, Y. (2009). "Persistent sand bars explained by geodynamic effects." *Hydrology And Land Surface Studies,* 36(1).

Stark, N., Coco, G., Bryan, K. R., and Kopf, A. (2012). "In-Situ Geotechnical Characterization of Mixed-Grain-Size Bedforms Using A Dynamic Penetrometer." *Journal of Sedimentary Research*, 82(7), 540–544.

Stark, N., Kopf, A., Hanff, H., Stegmann, S., and Wilkens, R. (2009). "Geotechnical investigations of sandy seafloors using dynamic penetrometers." *IEEE/MTS Oceans 2009*, Biloxi, MS, 1–10.

Stark N., Hay, A.E., and Trowse, G. (2014a). "Geotechnical investigation of areas of difficult access using portable free-fall penetrometers," *Proc., CPT'14*, Las Vegas, NV.

Stark N., Staelens P., Hay, A.E., Hatcher, B., and Kopf, A. (2014b). "Cost-effective Geotechnical and Sedimentological Early Site Assessment for Ocean Renewable Energies," *IEEE/MTS Oceans 2014*, St. John's, NL, 1-8.

Stoll, R. D., and Akal, T. (1999). "XBP - Tool for rapid assessment of seabed sediment properties." *Sea Technol.* (40), 47–51.

Stoll, R. D., Sun, Y.F., and Bitte, I. (2007). "Seafloor properties from penetrometer tests." *J. Ocean. Eng.* (32), 57–63.

Yehle, L.A. (1971). "Reconnaissance Engineering Geology of the Yakutat Area, Alaska, With Emphasis on Evaluation of Earthquake and Other Geologic Hazards." *Geological Survey Professional Paper 1074.* USGS.